The EMBO Journal (2009) 28, 926–936 | © 2009 European Molecular Biology Organization | All Rights Reserved 0261-4189/09
www.embojournal.org

THE EMBO JOURNAL

The transcription factor OsNAC4 is a key positive regulator of plant hypersensitive cell death

Takashi Kaneda[1,3], Yuri Taga[2,3], Ryota Takai[1], Megumi Iwano[1], Hiroyoshi Matsui[2], Seiji Takayama[1], Akira Isogai[1] and Fang-Sik Che[1,2,*]

[1]Graduate School of Biological Sciences, Nara Institute of Science and Technology (NAIST), Takayama Ikoma, Nara, Japan and [2]Graduate School of Bio-Science, Nagahama Institute of Bio-Science and Technology, Tamura Nagahama, Shiga, Japan

The hypersensitive response (HR) is a common feature of plant immune responses and a type of programmed cell death. However, little is known about the induction mechanism of HR cell death. We report that overexpression of *OsNAC4*, which encodes a plant-specific transcription factor, leads to HR cell death accompanied by the loss of plasma membrane integrity, nuclear DNA fragmentation and typical morphological changes. In *OsNAC4* knock-down lines, HR cell death is markedly decreased in response to avirulent bacterial strains. After induction by an avirulent pathogen recognition signal, OsNAC4 is translocated into the nucleus in a phosphorylation-dependent manner. A microarray analysis showed that the expression of 139 genes including *OsHSP90* and *IREN*, encoding a Ca^{2+}-dependent nuclease, were different between the *OsNAC4* knock-down line and control line during HR cell death. During the induction of HR cell death, OsHSP90 is involved in the loss of plasma membrane integrity, whereas IREN causes nuclear DNA fragmentation. Overall, our results indicate that two important events occurring during HR cell death are regulated by independent pathways.

The EMBO Journal (2009) **28,** 926–936. doi:10.1038/emboj.2009.39; Published online 19 February 2009
Subject Categories: differentiation & death; plant biology
Keywords: HR cell death; OsNAC4; phosphorylation; plant immune response; transcription factor

Introduction

Plants are continuously confronted with diverse potential pathogens; as a result, these organisms have evolved intricate immune mechanisms to recognize and defend themselves against a wide array of disease-causing agents (Jones and Dangl, 2006). One of the most efficient and immediate immune responses is hypersensitive response (HR) cell death (Lam, 2004). HR is characterized by rapid, localized death of plant cells at the site of pathogen infection (Lam, 2004). HR cell death requires active plant metabolism and intact transcriptional and translational machinery in the host plant (Richberg *et al*, 1998). The induction of HR is associated with signalling events, such as protein phosphorylation and the generation of reactive oxygen species (Alvarez *et al*, 1998). Spontaneous activation of HR cell death in the absence of pathogens has been reported in transgenic plants expressing foreign genes (Mittler *et al*, 1995), suggesting that HR cell death is a form of programmed cell death (PCD).

HR cell death shows morphological and biochemical traits similar to animal apoptosis, the most characterized form of PCD. These common features include plasma membrane shrinkage and condensation, loss of plasma membrane integrity and nuclear DNA fragmentation resulting from internucleosomal cleavage (Che *et al*, 1999; Tanaka *et al*, 2001; Yao *et al*, 2001). Despite these morphological and biochemical similarities, several characteristics differ between these two forms of PCD. Apoptotic bodies, which in animal cells are phagocytosed by other cells, are not formed during plant HR cell death, because of the presence of a cell wall. Whole-genome sequencing has revealed that plants lack obvious homologues to key proteins involved in animal apoptosis, such as Bcl-2 family proteins (Kutuk and Basaga, 2006) or caspases (Shi, 2002). In addition, vacuoles, which are multifunctional plant cell organelles, have an important function in plant PCD, with a key role for vacuolar processing enzyme (Hatsugai *et al*, 2004). Although the existence of HR cell death in plants has been recognized for many years, a description of the molecular players that serve as the central executioners has remained elusive.

Acidovorax avenae is a Gram-negative bacterium that causes a seedling disease characterized by the formation of brown stripes on the sheaths of infected plants. The host range of *A. avenae* is wide among monocotyledonous plant; however, individual strains of the pathogen infect only one or a few host species (Kadota *et al*, 1996). For example, strains isolated from rice such as K1 can infect only rice plant (virulent), whereas N1141 strain isolated from finger millet cannot infect rice even after being inoculated into rice tissues (avirulent). We recently reported that an avirulent N1141, but not virulent strains such as H8301 or K1, induced immune responses in rice, including rapid cell death, oxidative burst, and transcription of several immune-related genes. This rapid cell death in rice cells induced by the avirulent strains or its flagellin, a component of the bacterial flagellum filament, was dependent on *de novo* protein synthesis (Che *et al*, 2000; Kaneda *et al*, 2007), accompanied by clear 180-bp nucleosomal DNA laddering and typical cell morphological changes, such as plasma membrane shrinkage and nuclear condensation (Che *et al*, 1999; Tanaka *et al*, 2001). These results suggest that the avirulent N1141 strain of *A. avenae* induces HR cell death in rice, which possesses all of the features that are characteristic of this process in plants.

*Corresponding author. Graduate School of Bioscience, Nagahama Institute of Bio-Science and Technology, 1266, Tamura Nagahama, Shiga 526-0829, Japan. Tel.: +81 749 64 8162; Fax: +81 749 64 8140; E-mail: k_sai@nagahama-i-bio.ac.jp
[3]These authors contributed equally to this work

Received: 22 August 2008; accepted: 23 January 2009; published online: 19 February 2009

We previously identified several genes that are upregulated during HR cell death using PCR subtraction analysis and microarray analysis. Among the identified genes, the *OsNAC4* gene encoding a plant-specific transcription factor (Ooka *et al*, 2003) was identified in both analyses. The *OsNAC4* transcript was induced 3 h after incubating with the N1141 strain or its flagellin, and expression levels at 6 h after inoculation were 30-fold higher than levels before inoculation (Fujiwara *et al*, 2004; Kaneda *et al*, 2007). The activation of *OsNAC4* mRNA expression did not occur when rice cells were inoculated with the strain lacking the ability to undergo HR cell death, suggesting that induction of *OsNAC4* is involved in HR cell death induction (Kaneda *et al*, 2007). OsNAC4 has a consensus sequence known as the NAC domain (petunia NAM and *Arabidopsis* ATAF1 and CUC2) (Souer *et al*, 1996; Collinge and Boller, 2001). The finding that petunia plants with mutated *NAM* genes failed to form shoot apical meristems indicated that NAM plays a role in determining the position of the shoot apical meristem and primordial in this plant (Souer *et al*, 1996). A few *NAC* genes, such as *AtNAC072* (*RD26*), *AtNAC019* and *AtNAC055* from *Arabidopsis* (Fujita *et al*, 2004), and *BnNAC* from *Brassica* (Hegedus *et al*, 2003), were found to be involved in the response to various environmental stresses. However, the exact role of OsNAC4 transcriptional factor has remained unclear.

In this study, we present the induction mechanism of plant HR cell death mediated by OsNAC4. Our results show that OsNAC4 is involved in the induction of HR cell death and may control the transcription of multiple genes, including *OsHSP90* and *IREN*. During the induction of HR cell death, Os HSP90 was involved in the loss of plasma membrane integrity, whereas IREN caused the cleavage of nuclear DNA. We propose a model in which the induction of HR cell death is regulated by a transcriptional network controlled by OsNAC4.

Results

Identification of OsNAC4 as HR cell death inducing transcription factor

To determine the role of OsNAC4 in the induction of HR cell death in rice, we developed a transient assay in cultured rice cells based on the *Arabidopsis* transient assay system (Mindrinos *et al*, 1994). Using particle gun bombardment, two plasmids were co-introduced into cultured rice cells, one of which encoded the *OsNAC4* gene and the other contained the *uidA* gene that encodes β-glucuronidase (GUS). Both the *OsNAC4* and *uidA* genes were under the control of the constitutive ubiquitin promoter derived from maize (Cornejo *et al*, 1993). If *OsNAC4* overexpression induces cell death, little GUS activity would accumulate in the transformed cultured rice cells. If overexpression does not induce cell death, transformed cells would exhibit high levels of GUS activity.

As shown in Figure 1A, the same GUS activity levels were detected in both *OsNAC4* plus *uidA* co-introduced cells (*OsNAC4*/*uidA* cells) and control *uidA* bombarded cells after 4 h transformation. GUS activity in *OsNAC4*/*uidA* cells was reduced by 16 h after transformation, and minimal accumulation of GUS activity was observed 24 h after transformation compared with that in control cells (Figure 1A). A similar *OsNAC4*-mediated reduction in GUS activity was also

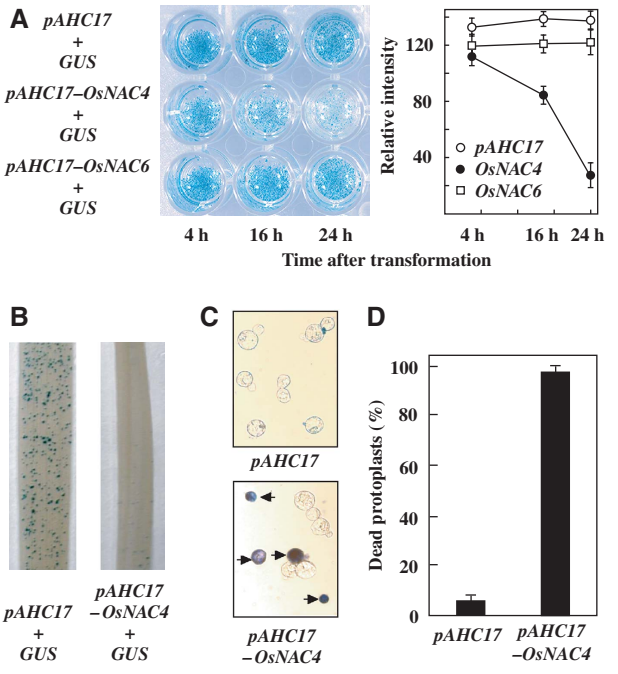

Figure 1 Cell death induction by *OsNAC4*. (**A**) Cell death was induced in cultured rice cells by co-introduction of *OsNAC4* gene (*pAHC17-OsNAC4*) or *OsNAC6* (*pAHC17-OsNAC6*) and *GUS*. After transformation by particle bombardment, GUS activity in each cell was detected histochemically. The relative intensity of GUS staining is shown in the right graph. The mean values with error bars were derived from 10 independent experiments. (**B**) GUS activity in a rice leaf 24 h after transformation. GUS activity was measured after co-introduction of *OsNAC4* (*pAHC17-OsNAC4*) and *GUS* (right) or *GUS* alone (left). *pAHC17* was used for control experiments. The experiments were carried out in three different biological materials. (**C**) Protoplasts were transfected with the *pAHC17* (control) or *pAHC17-OsNAC4* vectors. After 12 h, protoplasts were incubated in 0.05% Evans blue for 5 min. (**D**) Protoplasts were transfected with *pAHC17* (control) or *pAHC17-OsNAC4*. Twelve hours after transfection, dead protoplasts were scored using a light microscope. Values on the y-axis describe the percentage of dead cell in transfected protoplasts. Each determination was done with at least 1000 cells in each experiment. The mean values with error bars were derived from five independent experiments.

observed in rice leaves (Figure 1B). To confirm that the reduction in GUS activity was a measure of cell death, we introduced an *OsNAC4* expression vector into protoplasts prepared from cultured rice cells, and then measured cell death using Evans blue, a marker of plasma membrane integrity. Dead protoplasts accumulated the dye, whereas live protoplasts excluded the dye (Figure 1C). After transient overexpression of *OsNAC4* in rice protoplasts, almost 100% of the protoplast population was scored as dead, whereas the death rate in vector control bearing cells was as low as 10% (Figure 1D).

Another important feature of HR cell death is nuclear DNA fragmentation (Che *et al*, 1999; Yao *et al*, 2001). Typically, terminal deoxynucleotidyl transferase-mediated dUTP nick-end labelling (TUNEL), which labels the free 3′-OH groups of DNA, is used to quantify DNA fragmentation and breakage (McCabe *et al*, 1997). Gold particles for bombardment were coated with a mixture of *pAHC17-OsNAC4* and *pAHC17-DsRed* and then bombarded into cultured rice cells. Six hours after transformation, the *OsNAC4*-expressing cultured rice cells (DsRed-positive cells) exhibited fluorescein-derived

bright-green fluorescence of their nuclei, as detected by TUNEL (Figure 2A–D). We constructed a *DsRed*-fused *OsNAC4* expression vector and transformed it into cultured rice cells. TUNEL staining showed that *OsNAC4-DsRed* transformed cells had fluorescein-derived bright-green fluorescence signals. The positions of all bright-green signals coincided with DsRed signals (Figure 2E–H). In contrast, no bright-green fluorescence was observed in cultured rice cells transformed with *DsRed* alone (Figure 2I–L), indicating that *OsNAC4* overexpression causes rapid DNA fragmentation accompanied with HR cell death.

Suppression of HR cell death by RNA interference with OsNAC4

We selected a 501-bp region of *OsNAC4* cDNA that encodes the C-terminus for RNAi experiments. This contains the 3′UTR and the TAR region, which is necessary for the transcriptional activity of OsNAC4. To determine whether this sequence is specific or shares similarity with other sequences, we searched the full-length rice cDNA database using BLASTN for short, nearly exact matches to the selected 501-bp region. No close similarity was detected for any genes other than *OsNAC4*, and the next level of similarity was at $E = 0.039$. Hence, the RNAi strategy was designed to target the *OsNAC4* gene specifically.

We generated three lines of cultured rice cells carrying the *OsNAC4* RNAi construct (NR2-2, NR2-3 and NR2-4) and one control transformant carrying the empty vector. After inoculation of the avirulent strain N1141, HR cell death measured by Evans blue staining was markedly decreased in the three RNAi transformant lines (NR2-2, NR2-3 and NR2-4) compared with the control transformant line (Figure 3A). To test whether the decrease in HR cell death correlated with reductions in OsNAC4, we quantified OsNAC4 protein levels in all transformant lines using an anti-OsNAC4 antibody. Immunoblot analysis of wild-type cell extracts using an anti-OsNAC4 antibody specifically detected a protein migrating with an apparent molecular mass of 35 kDa (Figure 3B; Supplementary Figure S1). The cell lines with decreased HR cell death, NR2-2, NR2-3 and NR2-4, exhibited 10-fold or greater reductions in OsNAC4 protein levels. In addition, the level of reduction in HR cell death was strongly associated with a reduction in OsNAC4 protein accumulation (Figure 3B).

We evaluated DNA fragmentation in *OsNAC4* knock-down and control lines after inoculation with the avirulent N1141 strain. TUNEL staining of NR2-4 RNAi transformants did not produce fluorescent nuclei (Figure 3C), whereas control cells exhibited multiple intensely stained nuclei 12 h after inoculation (Figure 3C). We also examined the percentage of TUNEL-positive nuclei in the above experiment. In the control line inoculated with the avirulent strain, approximately 19% of nuclei had FITC-derived fluorescence 12 h after inoculation (Figure 3D). In contrast, approximately 2% of TUNEL-positive nuclei were detected in the N1141-inoculated NR2-4 line (Figure 3D).

We next studied the ultrastructure of NR2-4 and control cells undergoing the induction of HR cell death using transmission electron microscopy. Mock-inoculated cells contained regularly shaped nuclei with an intact nuclear envelope (Figure 4A), and the cytoplasm showed a highly ordered structure (Figure 4D). Twelve hours after inoculation of the avirulent strain, control cells had nuclei undergoing HR cell death that exhibited an irregular shape with invaginations and an electron-dense structure that may have resulted from chromatin condensation (Figure 4B). The plasma mem-

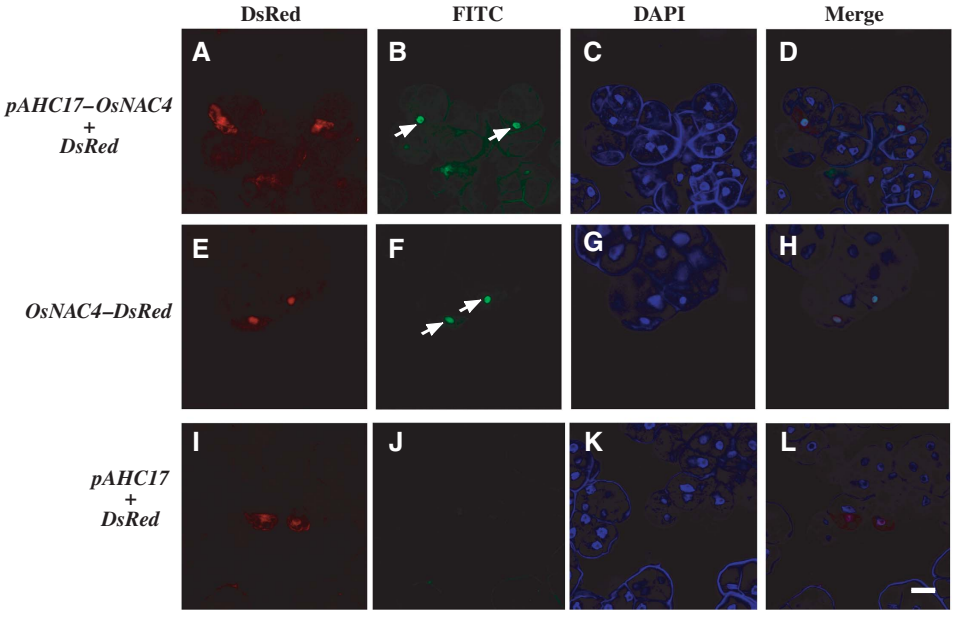

Figure 2 DNA fragmentation detected by TUNEL staining. (**A**–**D**) Cell images of cultured rice cells transfected with *OsNAC4* and *DsRed*. (**E**–**H**) Cell images of cultured rice cells transfected with *DsRed*-fused with *OsNAC4*, *OsNAC4-DsRed*. (**I**–**L**) Cell images of cultured rice cells transfected with *pAHC17* (empty vector) and *DsRed*. (A, E, I) are DsRed images, (B, F, J) are FITC images, (C, G, K) are DAPI images and (D, H, L) are merged images. The arrows indicate the TUNEL-positive nucleus. At least 200 transformed cells for each experiment were observed in three different biological materials. Ninety-five percent out of the *OsNAC4* or *OsNAC4-DsRed* expressing cultured rice cells possessed TUNEL positive nuclei. Bar represents 10 μm.

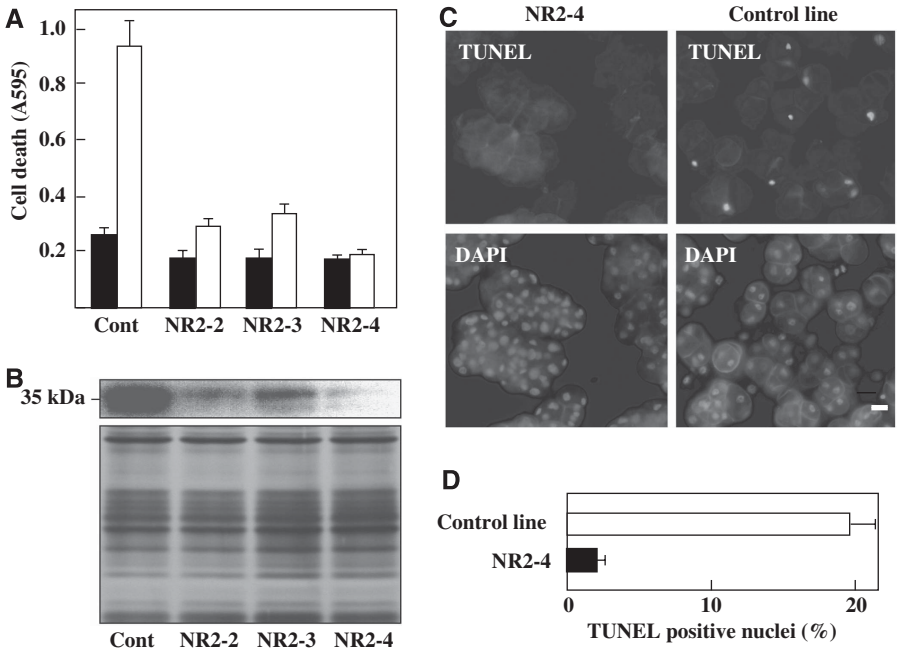

Figure 3 Suppression of HR cell death in *OsNAC4* RNAi transformants. (**A**) Cell death detected by Evans blue staining in *OsNAC4* RNAi transformant lines (NR2-2, NR2-3 and NR2-4) before (solid column) and 8 h after (open column) inoculation with the avirulent N1141 strain. (**B**) Accumulation of OsNAC4 was detected with an anti-OsNAC4 antibody in *OsNAC4* RNAi knock-down lines. Proteins (10 μg) from vector transformed cells (Cont) and RNAi transformant lines were separated on a 12.5% (w/v) SDS–PAGE and transferred to a nitrocellulose membrane. Then OsNAC4 were detected by immunoblotting with an anti-OsNAC4 antibody (top part). The same amount of each fraction was separated by SDS–PAGE and proteins were detected by silver staining (lower part). (**C**) DNA fragmentation in *OsNAC4* knock-down (left panels) and control (right panels) lines was assessed after inoculation with the avirulent N1141 strain. TUNEL (upper panels) and DAPI (lower panels) staining are shown. Bar represents 10 μm. (**D**) Percentage of TUNEL-positive nuclei in NR2-4 and vector transformed lines (control line) inoculated with N1141. The percentage of TUNEL-positive nuclei was determined by counting nuclei within 20 individual fields. Each determination was done with at least 2000 nuclei in each of three independent experiments. A full colour version of this figure is available at *The EMBO Journal* online.

brane also appeared to have partially separated from the cell wall (Figure 4E). In contrast, these morphological changes in the nucleus and plasma membrane were not observed when the *OsNAC4*-deficient line NR2-4 was inoculated with the avirulent strain (Figure 4C and F). From these observations, we concluded that OsNAC4 is a key transcription factor regulating the induction of HR cell death in rice.

Translocation of OsNAC4 into the nucleus depends on phosphorylation

As H_2O_2 is known as an important signalling molecule for HR induction, we analyzed the generation of H_2O_2 in *OsNAC4*-RNAi cultured cells. When the incompatible flagellin was added to cultured rice cells, rapid H_2O_2 generation was observed (Supplementary Figure S2). The same generation pattern of H_2O_2 was also observed in *OsNAC4*-RNAi NR2-4 cells even when HR cell death was abolished (Supplementary Figure S2), suggesting that OsNAC4 is located down-stream of H_2O_2 signals in the HR induction pathway.

We next examined whether induction of OsNAC4-mediated cell death in cultured rice cells is involved in protein phosphorylation signalling. For this purpose, staurosporine, a potent inhibitor of plant and animal serine/threonine protein kinases, was used. In the absence of staurosporine, cell death induced by the avirulent N1141 strain was detected by Evans blue staining 6 h after inoculation, and the number of dead cells gradually increased. Conversely, HR cell death was completely blocked by staurosporine treatment (2 μM) for up to 9 h after inoculation (Figure 5A). During this experimental period, bacterial growth rates were the same in the presence and absence of 2 μM staurosporine.

To clarify whether OsNAC4-mediated HR cell death is also inhibited by staurosporine, protoplasts overexpressing *OsNAC4* were treated with staurosporine and then examined for the inhibition of cell death by Evans blue. A large proportion of dead cells were observed in cells overexpressing *OsNAC4*; staurosporine reduced the amount of cell death (Figure 5B). To study the step in OsNAC4-induced cell death that required protein phosphorylation, we examined the effects of staurosporine on *OsNAC4* mRNA expression using quantitative real-time RT–PCR in cultured rice cells inoculated with the avirulent N1141 strain. The *OsNAC4* induction kinetics after inoculation with the N1141 strain was unaffected by the addition of staurosporine (Figure 5C), suggesting that inhibition of protein phosphorylation does not influence the induction of *OsNAC4* mRNA during HR cell death.

We next examined the subcellular localization of OsNAC4 during HR cell death induction by immunoblot analysis. Inoculation with the avirulent strain increased the amount of endogenous OsNAC4 protein in the nuclear fraction in a time-dependent manner, whereas treatment with water alone did not affect the proportion of OsNAC4 in the nuclear fraction (Figure 6A). The amount of OsNAC4 within the cytosolic fraction was slightly decreased by avirulent N1141 inoculation (Figure 6A). Moreover, the total amount of

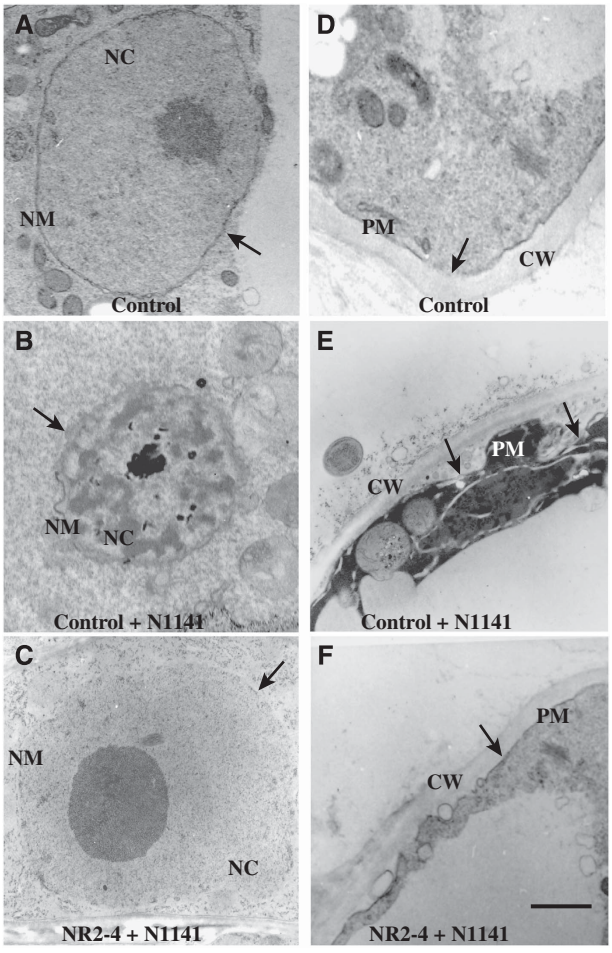

Figure 4 Morphological analysis using transmission electron microscopy. (**A**) A nucleus in a cell transformed with empty vector (control cell) 12 h after water treatment. The arrow indicates a normal nucleus. (**B**) A nucleus in empty vector-transformed cells (control cell) 12 h after inoculation with the avirulent N1141 strain. The arrow indicates condensed nucleus. (**C**) A nucleus in the *OsNAC4* knock-down NR2-4 line after a 12-h inoculation with the avirulent N1141 strain. The arrow indicates a normal nucleus. (**D**) The cell wall and plasma membrane in a cell transformed with empty vector (control cell) 12 h after water treatment. The arrow indicates a normal plasma membrane. (**E**) The cell wall and plasma membrane in empty vector transformed cells (control cell) 12 h after inoculation with the avirulent N1141 strain. The arrows indicate the separated-plasma membrane from the cell wall. (**F**) The cell wall and plasma membrane in the *OsNAC4* knock-down NR2-4 line after a 12-h inoculation with the avirulent N1141 strain. The arrow indicates a normal plasma membrane. CW, cell wall; NC, nucleus; NM, nuclear membrane; PM, plasma membrane. Bar represents 1 μm.

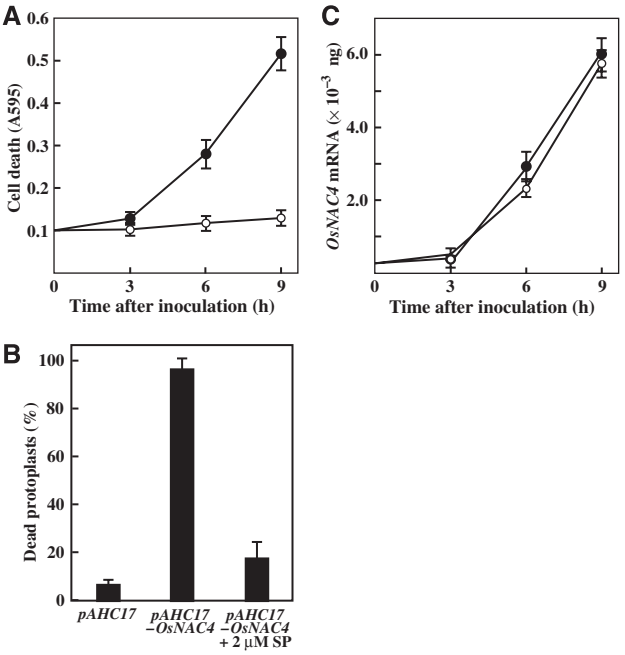

Figure 5 Effects of protein phosphorylation on OsNAC4-mediated cell death. (**A**) Time-course of cell death in cultured rice cells after inoculation with the avirulent N1141 strain in the presence of 2 μM staurosporine (open circles) or absence of the inhibitor (solid circles). The amount of cell death was estimated by Evans blue staining of individual cells at 595 nm. Each data point represents the average of three independent experiments. Bars indicate the standard errors. (**B**) Cell death in protoplasts transfected with the *pAHC17* (control) and *pAHC17-OsNAC4* vectors in the presence or absence of 2 μM staurosporine. Protoplasts were treated with staurosporine concurrent with transfection. Twelve hours after transfection, dead protoplasts were scored using a light microscope. Y-axis values represent the percentage of transfected protoplasts that were determined to be dead. Each data point represents the average of three independent experiments. Bars indicate the standard errors. (**C**) Time-dependent accumulation of *OsNAC4* mRNA in cultured rice cells after inoculation with the avirulent N1141 strain of *A. avenae* in the presence (open circles) or absence (closed circles) of 2 μM staurosporine. The amount of each mRNA was measured by real-time RT–PCR; these values were calculated from the threshold point located in the log-linear range of RT–PCR. Quantification of each *OsNAC4* mRNA was calculated with calibration curve, which was prepared using standard *OsNAC4* genes of known template amounts and corrected with reference data of *Act-1* gene. Each data point represents the average of three independent experiments. Bars indicate the standard errors.

OsNAC4 protein in whole cells was slightly increased during HR cell death induction (data not shown). We also examined the nuclear translocation of OsNAC4 in cultured rice cells inoculated with the virulent K1 strain. Western blot analysis showed that OsNAC4 does not translocate into nuclei during the compatible interactions (data not shown).

Immunogold electron microscopy also showed that gold particles were equally distributed in the cytosol and nucleus before inoculation (Figure 6B), whereas cells undergoing HR cell death had a greater proportion of gold particles in the nucleus than in the cytosol (Figure 6B). Quantitative analysis showed that about 85% of the total number of gold particle was in the nucleus in cells undergoing HR cell death (Figure 6C). In NR2-4 cells transformed with the *OsNAC4* RNAi construct, minimal numbers of gold particles were found in both the nucleus and cytosol (Figure 6B and C), and the number of particles did not increase during the incompatible interaction (Figure 6C). Preimmune serum did not produce any appreciable binding of gold particles, and omission of the primary antibody also yielded negative results (Figure 6B).

To clarify whether the nuclear translocation of OsNAC4 in rice cells is necessary for the induction of HR cell death, the localization of NES (nuclear export signal)-containing OsNAC4 and its HR induction activity were examined. cDNA encoding the NES sequence (Leu-54 to Gln-69) was

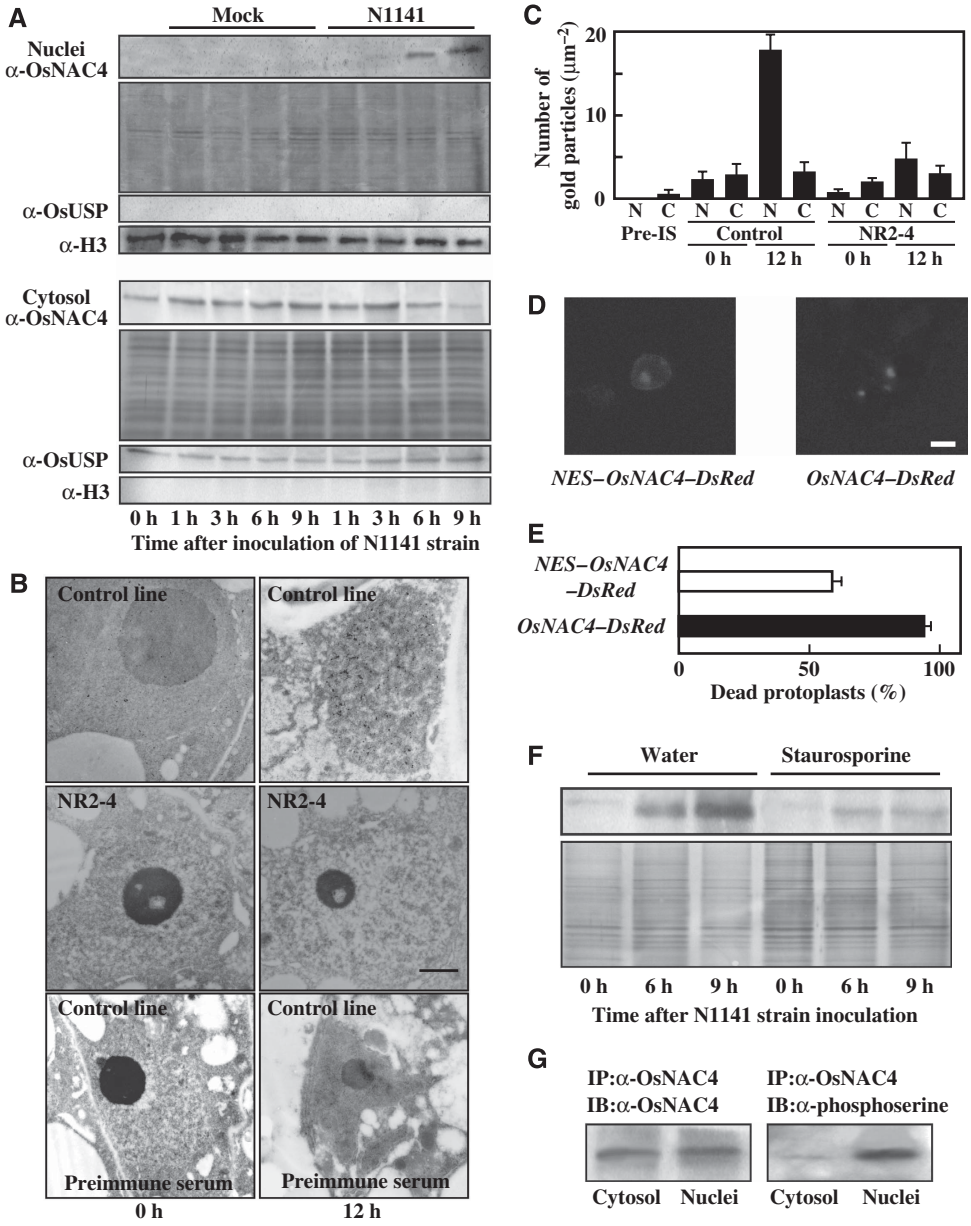

Figure 6 Translocation of OsNAC4 into the nucleus and phosphorylation of OsNAC4 during HR cell death. (**A**) Time-dependent accumulation of OsNAC4 in cultured rice cells after inoculation with the avirulent N1141 strain. The upper panels represent the amount of OsNAC4 protein in the nuclear fraction. Nuclear fractions (10 μg protein) were separated by SDS–PAGE and transferred to a nitrocellulose membrane. Then OsNAC4 were detected by immunoblotting with an anti-OsNAC4 antibody (top part). The same amount of each nuclear fraction was separated by SDS–PAGE and proteins were detected by silver staining (middle part). The lower panel represents the proportion of OsNAC4 in the cytosolic fraction. Total protein (10 μg) from each fraction was separated by SDS–PAGE and transferred to a nitrocellulose membrane. Then OsNAC4 were detected by immunoblotting with an anti-OsNAC4 antibody (upper part). The same amount of each cytosolic fraction was separated by SDS–PAGE and proteins were detected by silver staining (lower part). The purity of each fraction was analysed by immunoblotting using an antihistone H3 antibody (nucleus-specific antibody) and an anti-OsUSP (cytosol-specific antibody). (**B**) Immunogold labelling of OsNAC4 using anti-OsNAC4 antibody. A control cell line (upper panels) and the NR2-4 OsNAC4 knock-down line (middle panels) were visualized 0 h (left panels) and 12 h (right panels) after inoculation with the avirulent N1141 strain. A control cells treated with preimmune serum were visualized 0 h (left panels) and 12 h (right panels) after inoculation with the N1141 strain (lower panels). Bar represents 1 μm. (**C**) The number of gold particles in the nucleus and cytosol when the OsNAC4 protein was immunogold labelled. The number of gold particles in nucleus and cytosol were visually counted. Pre-IS, preimmune serum; N, nucleus; C, cytosol. Each data represent the average of the particle number in five counted area (1 μm^2). Bars indicate the standard errors. (**D**) The localization of *NES*-fused *OsNAC4-DsRed* and *OsNAC4-DsRed* after 6 h transformation in rice protoplasts. *NES* fused to the N-terminal of *OsNAC4-DsRed* (left panel) and *OsNAC4-DsRed* (right panel). Bar represents 10 μm. (**E**) Cell death in protoplasts transfected with the *NES-OsNAC4-DsRed* and *OsNAC4-DsRed* (control) vectors. Six hours after transfection, dead protoplasts were scored using a light microscope. Y-axis values represent the percentage of transfected protoplasts that were determined to be dead. Each determination was done with at least 200 cells in each of three independent experiments. Bars indicate the standard errors. (**F**) The time-dependent accumulation of OsNAC4 in nuclei isolated from cultured rice cells after inoculation with the avirulent N1141 strain. The left three lanes represent nuclear OsNAC4 in water-treated cells, whereas the right three lanes represent OsNAC4 in cells treated with 2 μM staurosporine. Total protein (10 μg) from each fraction was separated by SDS–PAGE and transferred to a nitrocellulose membrane. The same amount of each fraction was separated by SDS–PAGE, and proteins were detected by silver staining (lower part). (**G**) Phosphorylation of the OsNAC4 protein accumulated in nuclei. Rice protoplasts were expressed with OsNAC4 and cytosol and nuclei fractions were isolated. Both protein extracts were subjected to immunoprecipitation (IP) with anti α-OsNAC4, and the same amounts of immunoprecipitated proteins were immunoblotted (IB) with the indicated antibodies. A full colour version of this figure is available at *The EMBO Journal* online.

cloned from rice *OsNAP1* (nucleosome assembly protein 1) and the cDNA encoding the NES was fused with the *OsNAC4-DsRed* gene and then placed under the control of the constitutive ubiquitin promoter from maize (Dong *et al*, 2005). The construct was introduced into rice protoplasts, and transient expression was observed by fluorescence microscopy. The OsNAC4-DsRed protein localized in the nucleus, whereas the NES-fused OsNAC4-DsRed localized in both the cytoplasm and nucleus (Figure 6D). Evans blue staining showed that approximately 100% of *OsNAC4-DsRed* transformed protoplasts were dead, whereas the death rate in the *NES*-fused *OsNAC4-DsRed*-bearing cells was as low as 60% (Figure 6E), suggesting that the accumulation of OsNAC4 in nuclei is involved in the initiation of HR cell death.

We next examined whether the protein phosphorylation is involved in OsNAC4 translocation into the nucleus. Cultured rice cells were inoculated with the avirulent N1141 strain in the absence or presence of 2 μM staurosporine; nuclei were subsequently isolated from each cultured rice cell. OsNAC4 clearly accumulated in the nuclear fraction in water-treated control cells, whereas staurosporine treatment decreased OsNAC4 accumulation in nuclei (Figure 6F). To examine the phosphorylation status of nuclear OsNAC4, phosphorylated OsNAC4 in the nuclear and cytosol fractions were detected in rice protoplasts transfected with an *OsNAC4*-expression vector using an antiphosphoserine antibody. The cytosol and nuclei proteins were subjected to immunoprecipitation with anti-OsNAC4 antibody and the immunoprecipitated protein extracts were immunoblotted with the anti-OsNAC4 antibody and antiphosphoserine antibody. Although OsNAC4 was evenly distributed between the nuclear and cytosolic fractions, phosphorylated OsNAC4 could only be observed in the nuclear fraction (Figure 6G). Therefore, the translocation of OsNAC4 into the nucleus may thus be regulated by OsNAC4 phosphorylation.

Identification of genes that are differentially expressed between the OsNAC4 knock-down and control lines during the incompatible interaction

To understand the molecular mechanisms by which OsNAC4 mediates cell death, 22 000 elements oligonucleotide microarray were used to analyze global gene expression changes in the *OsNAC4*-RNAi cell line NR2-4, with a control line inoculated with N1141 strain and water at 0, 1, 3 and 6 h. Equal amounts of Cy3-labeled cRNA prepared from the water-treated control line and Cy5-labeled cRNA prepared from the N1141-inoculated control line were applied to a microarray slide. Similarly, Cy3-labeled and Cy5 labeled cRNAs were prepared from water-treated and N1141-inoculated *OsNAC4* RNAi NR2-4 line. The microarray analysis used was RNAs prepared from three different biological samples and hybridization was carried out twice with each RNA sample. Two-way analysis of variance (ANOVA) identified 3288 genes that showed statistically significant expression changes in N1141 inoculated both cell lines. We next identified genes that were differentially expressed between the NR2-4 and control cell lines during HR cell death. A *t*-test ($P<0.01$) revealed that 139 of 3288 genes were expressed differently between the NR2-4 and control lines during HR cell death (Supplementary Table S1). The most abundant of these 139 gene transcripts were involved in metabolism (15.6%), transcription (12.0%) and signal transduction (10.6%) (Supplementary Figure S3A). All genes were upregulated in the control line after inoculation of the avirulent N1141 strain, indicating that *OsNAC4* positively regulates the expression of these genes.

Role of OsHSP90 in HR cell death

We sought to identify candidate genes that are involved in the induction of HR cell death from 139 genes. Functional prediction analyses of all 139 genes showed that *AK102478* encodes rice heat-shock protein 90 (OsHSP90). HSP90 is an essential and abundant molecular chaperone in both plants and animals and modulates numerous signal transduction pathways that regulated plant immune responses. Therefore, we chose the *AK102478* gene encoding HSP90 as a potential target of OsNAC4 involved in HR cell death. This gene was upregulated in the early stages of plant immune responses induced by avirulent N1141 strain inoculation; this induction was completely abolished in an *OsNAC4* RNAi knock-down mutant (Supplementary Table S1). Real-time RT–PCR analysis revealed that the *OsHSP90* transcript was induced 2 h after inoculation with the avirulent N1141 strain and maintained up to 6 h after incubation, whereas *OsHSP90* mRNA levels were not increased by inoculation of the virulent K1 strain (Figure 7A). To identify the subcellular localization of OsHSP90, we generated a *GFP*-fused *OsHSP90* expression vector and *DsRed*-fused AtbZIP28 (which is known to be efficiently delivered into the ER: Tajima *et al*, 2008), and cotransformed both vectors to cultured rice cells. All bright-green signals (OsHSP90) colocalized with DsRed signals (Figure 7B), indicating that OsHSP90 localizes to the ER.

To examine the role of OsHSP90 in the induction of cell death, we constructed an *OsHSP90* expression vector, which we introduced into protoplasts prepared from cultured rice cells. Evans blue staining showed that approximately 80% of the transformed protoplasts were dead, whereas the death rate in *pAHC17* (control vector)-bearing cells was as low as 10% (Figure 7C). Geldanamycin (GDA) is specific inhibitor of HSP90 that affects its ATPase activity by binding to the conserved N-terminal domain (Picard, 2002; Takabatake *et al*, 2007). GDA treatment completely suppressed the loss of plasma membrane integrity, but not DNA fragmentation (data not shown), in both *OsHSP90*- and *OsNAC4*-overexpressing protoplasts (Figure 7C). These results indicate that the upregulation of *OsHSP90* induced by OsNAC4 is required for cell death evidenced by loss of plasma membrane integrity.

DNA fragmentation, another marker of OsNAC4-induced cell death was analyzed in OsHSP90 overexpressing cells using TUNEL. Unexpectedly, no DNA fragmentation in cultured rice cells cotransformed with *OsHSP90* and *DsRed* was observed (Figure 7D), indicating that OsHSP90 is not involved in rapid nuclear DNA fragmentation during HR cell death.

Role of IREN in HR cell death

The DNA fragmentation detected by TUNEL staining should be involved in endonucleolytic enzyme(s) that can cleave dsDNA to produce 3′-hydroxyl termini. In plant PCD, increased activities of several nucleases have been reported; however, no plant endonucleases related to HR cell death have been identified. The analysis of sequence motifs in all 139 genes showed that only one cDNA encoded a putative

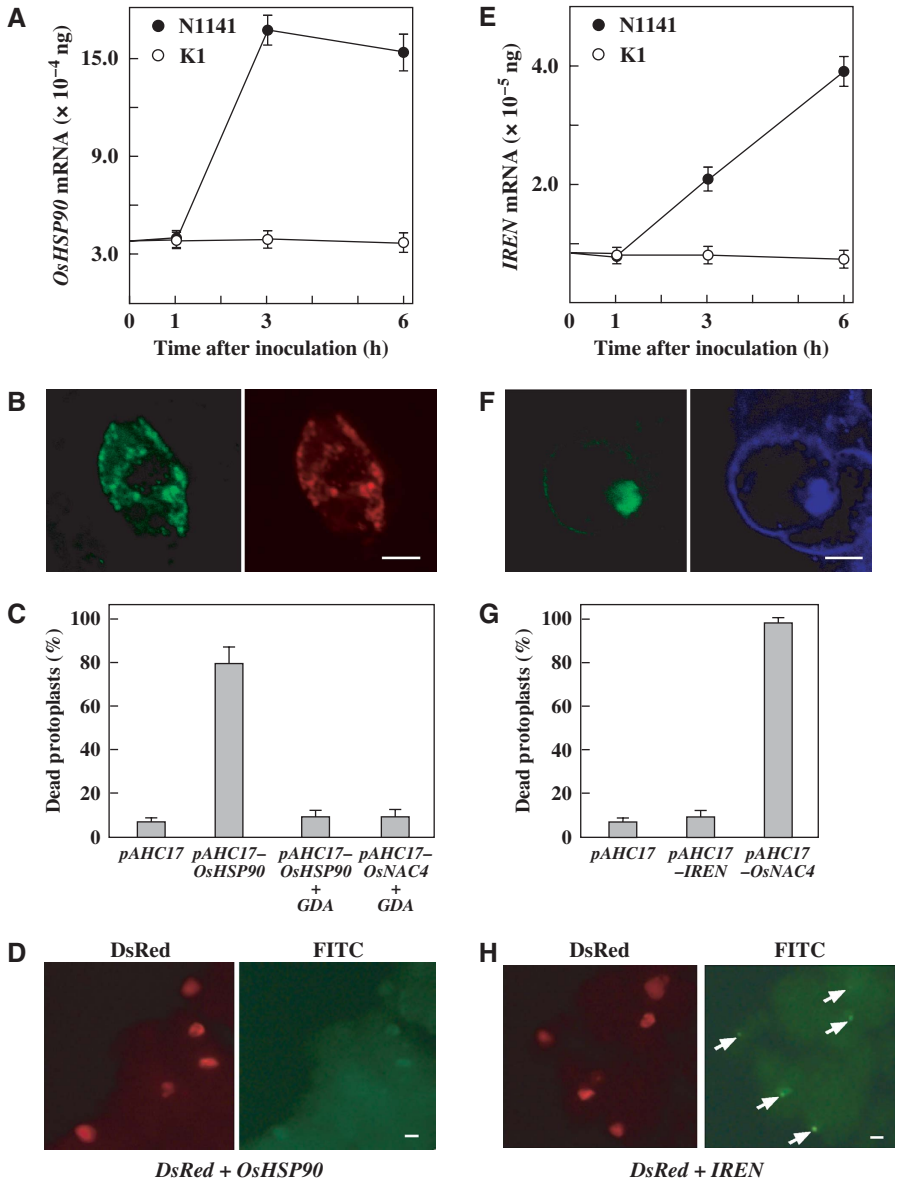

Figure 7 Contribution of OsHSP90 and IREN to HR cell death induction. (**A**) Time-course of *OsHSP90* expression in cultured rice cells after inoculation with the avirulent N1141 strain (solid circles) or the virulent K1 strain (open circles) of *A. avenae*. The amount of *OsHSP90* mRNA was measured by real-time RT–PCR. Each data point represents the average of three independent experiments. Bars indicate the standard errors. (**B**) Subcellular localization of GFP-fused OsHSP90. *GFP*-fused *OsHSP90* expression vector and *DsRed*-fused *AtbZIP28* (which is known to be efficiently delivered into ER: Tajima *et al*, 2008) cotransformed to cultured rice cells. The left panel represents GFP cell images, whereas the right panel displays DsRed images. Bar represents 10 μm. (**C**) Cell death in protoplasts transfected with *pAHC17* alone (control) or *pAHC17-OsHSP90* and *pAHC17-OsNAC4* in the presence and absence of GDA. Protoplasts were treated with GDA concurrently to transfection. Twelve hours after transfection, dead protoplasts were scored using a light microscope. Y-axis values represent the percentage of dead cell relative to the number of transfected protoplasts. Each data point represents the average of three independent experiments. Bars indicate the standard errors. (**D**) DNA fragmentation was detected by TUNEL in cultured rice cells cotransformed with *OsHSP90* and *DsRed*. The left panel represents DsRed cell images, whereas the right panel displays FITC images. Bar represents 10 μm. (**E**) Time-course of *IREN* expression in cultured rice cells after inoculation with the avirulent N1141 strain (solid circles) or the virulent K1 strain (open circles) of *A. avenae*. The amount of *IREN* mRNA was measured by real-time RT–PCR. Each data point represents the average of three independent experiments. Bars indicate the standard errors. (**F**) Subcellular localization of GFP-fused IREN. The left panel represents GFP cell images, whereas the right panel displays DAPI staining images. Bar represents 10 μm. (**G**) Cell death in protoplasts transfected with the *pAHC17* (control), *pAHC17-IREN* and *pAHC17-OsNAC4* vectors. Twelve hours after transfection, dead protoplasts were scored using a light microscope. Y-axis values represent the percentage of dead cell relative to the number of transfected protoplasts. Each data point represents the average of three independent experiments. Bars indicate the standard errors. (**H**) DNA fragmentation was detected by TUNEL in cultured rice cells cotransformed with *IREN* and *DsRed*. The left panel represents DsRed cell images, whereas the right panel displays FITC images. The arrow indicates a TUNEL-positive nucleus. Bar represents 5 μm.

endonuclease contained (*AK100514*). The product of this gene is a 470-amino acid protein with a calculated molecular mass of 54 658. It contains an endonuclease motif in the N-terminal region and an EF hand motif, which is a Ca^{2+}-binding site, in the C-terminal region (Supplementary Figure S3B). Real-time RT–PCR analysis with *IREN*-specific primer

sets showed that the avirulent N1141 strain induced expression of *IREN* mRNA within 6 h of inoculation, whereas the virulent K1 strain did not induce detectable *IREN* mRNA levels until 8 h after inoculation (Figure 7E). Therefore, we concluded that this endonuclease, designated *IREN* (immune-related endonuclease), is a candidate gene involved in the induction of DNA fragmentation in HR cell death.

To understand the role of *IREN* in HR-associated DNA fragmentation, we constructed a *GFP*-fused *IREN* expression vector and transformed the vector into cultured rice cells. The bright-green signals (OsHSP90) colocalized with the nuclei, which were identified by DAPI staining (Figure 7F), indicating that IREN is mainly localized in nuclei. We next cloned the full-length *IREN* cDNA into a vector under the control of the ubiquitin promoter (*pAHC17-IREN*), and introduced this construct into rice cells with the reporter plasmid *pAHC17-DsRed*. After TUNEL staining, all of the *IREN*-expressing cultured rice cells (DsRed-positive cells) exhibited fluorescein-derived bright-green fluorescence of their nuclei (Figure 7G), suggesting that *IREN* overexpression causes rapid DNA fragmentation in nuclei. We next examined whether IREN is involved in the loss of plasma membrane integrity by Evans blue staining. Overexpression of *OsNAC4* caused cell death, whereas no cell death induction was detected when *IREN* was transiently expressed in rice protoplasts (Figure 7H). The DNA fragmentation induced by exogenous *IREN* expression did not directly cause a loss of plasma membrane integrity.

Discussion

HR cell death induction mediated by OsNAC4

Genome-wide analyses revealed that 75 and 105 putative NAC proteins are present in the rice and *Arabidopsis thaliana* genomes, respectively. NAC proteins are classified into two large groups, groups I and II, based on structural features (Ooka *et al*, 2003). Group I can be divided into 14 subgroups based on similarities in their NAC domains, and OsNAC4 belongs to the group I-OsNAC3 subgroup. This subgroup includes nine NAC genes of rice, whereas no NAC genes of dicotyledonous plants such as *Arabidopsis* and tobacco exist in this subgroup (Ooka *et al*, 2003). These data argue that the molecular induction of cell death after OsNAC4 activation may be unique to monocotyledonous plants such as rice. However, exogenous expression of *OsNAC4* in *Nicotiana benthamiana* leaves by viral transduction resulted in lesions similar to those observed on rice plants after the induction of HR cell death (Supplementary Figure S4). These observations suggest that the *OsNAC4*-mediated molecular pathways governing HR cell death exist in both monocotyledonous plants and dicotyledonous plants such as tobacco. HR cell death induction in *Arabidopsis* and tobacco likely involves functional homologues of *OsNAC4*.

HR cell death may inhibit or delay further spread of the pathogen, but its role in plant immunity has been difficult to ascertain due to the lack of plant mutants affected solely in cell death. Experimental systems that combine *OsNAC4* RNAi knock-down transformants with pathogens have provided excellent models to answer such a question. Therefore, we tried to generate redifferentiated *OsNAC4* knock-down rice plants. Although more than 100 lines, including the three lines (NR2-2, NR2-3 and NR2-4) used in this paper, were used for these redifferentiation experiments, we could not obtain redifferentiated rice plants. OsNAC4 contributes not only to hypersensitive cell death but also to plant differentiation or plant regeneration.

H_2O_2 is known to be an important signal molecule for HR induction. When the incompatible flagellin was added to *OsNAC4*-RNAi line, the same H_2O_2 generation pattern was also observed (Supplementary Figure S1), even though HR cell death was abolished, suggesting that OsNAC4 is located down-stream of the H_2O_2 signal in the HR induction pathway. Moreover, real time RT–PCR analysis showed that the Copper Zinc Superoxide Dismutase 1 (*CSD1*) gene and Bax Inhibitor 1 (*BI-1*) gene (both genes are reported to be induced during the HR) were not induced in the *OsNAC4*-RNAi line upon infection with the incompatible N1141 strain. OsNAC4 might be upstream of these HR execution factors. A further experiment will be necessary to elucidate a role of OsNAC4 in the HR cell death induction.

Loss of plasma membrane integrity mediated by OsHSP90

We observed that transient expression of *OsHSP90* or *OsNAC4* led to a loss of plasma membrane integrity, as measured by Evans blue staining. Because *OsHSP90* expression was regulated by OsNAC4 in our cell system, this heat-shock protein may induce plasma membrane dysfunction. HSP90 is a highly conserved molecular chaperone in eukaryotes that is essential for the maturation and activation of many signalling proteins. HSP90 proteins constitute families, and our genome-wide analysis detected eight HSP90 genes in rice. Protein Subcellular Localization Prediction (PSORT) showed that among the eight HSP90 homologues, only the OsHSP90, in this study, localizes to the endoplasmic reticulum, whereas the others are located in the cytosol or nucleus. Similarly, seven homologues in Arabidopsis whole genome were included and only AtHSP90-7 (SHD/GRP94) was predicted to localize within the endoplasmic reticulum (Krishna and Gloor, 2001). AtHSP90-7 is responsible for the correct folding of a number of proteins that are destined for the plasma membrane. On the basis of the fact that OsHSP90 is a unique ER molecule, OsHSP90 is likely an ortholog of AtHSP90-7 and also responsible for the correct folding of plasma membrane proteins. Therefore, it is easily conceivable that any changes in OsHSP90 levels might result in plasma membrane disintegration.

Putative AtHSP90-7 othologs have been identified in higher plants, *Madafascar periwinkle* and barley. It was reported that these genes are slightly induced by heat shock, pathogen infection or cell culturing. Moreover, a mutation in AtHSP90-7 causes a pleiotropic phenotype, namely, expansion of the shoot apical meristem and floral meristem, disorganized cell arrangement in the root apical meristem and defects in pollen tube elongation. However, their target proteins and their biological functions have never been identified. Therefore, it is important to clarify the pleiotropic effects of OsHSP90 and the target proteins of OsHSP90 in the ER.

DNA fragmentation mediated by IREN

Elevation of cytosolic Ca^{2+} in the early stages of HR cell death has been observed in multiple plant species, including tobacco, soybeans and *Arabidopsis* (Levine *et al*, 1996). Ca^{2+} influx is thought to be both necessary and sufficient to

trigger HR cell death. Additional studies examining the magnitude, duration and localization of perturbations in Ca^{2+} distribution will likely determine signal specificity. The activation of the HR cell death program by sustained Ca^{2+} influxes may provide a selective cue that prevents inadvertent program activation by minor perturbations in either redox status or Ca^{2+} distribution. *IREN* encodes an endonuclease possessing an EF-hand motif; induction of this gene resulted in rapid nuclear DNA fragmentation. IREN is a candidate for an HR cell death-related factor that is activated by elevated intracellular Ca^{2+} concentrations. During thymocyte apoptosis, increases in cytosolic Ca^{2+} directly activate a Ca^{2+}-dependent endonuclease; similar events are implied in the induction of PCD in plants (Levine *et al*, 1996). Although overexpression of IREN induced DNA fragmentation (Figure 7F), it is not clear whether IREN is the only factor involved in the DNA fragmentation process in HR cell death.

A model of OsNAC4 action in HR cell death induction

Our data propose an attractive and simplified model for HR cell death induction. In the absence of pathogen recognition signals, the small amounts of constitutively expressed OsNAC4 are equally distributed to the cytoplasm and nucleus. We have confirmed this distribution using immunoelectron microscopy (Figure 6B and C). After an appropriate pathogen recognition signal is encountered, *OsNAC4* expression and phosphorylation are induced. OsNAC4 protein then accumulates in the cytosol, where it is phosphorylated and transported into the nucleus. Inside the nucleus, OsNAC4 is involved in the expression of at least 139 genes including *OsHSP90* and *IREN*. Although OsHSP90 is located in ER and appears to cause a loss of membrane integrity either directly or indirectly, IREN is translocated into nucleus where it cleaves nuclear DNA through its endonuclease activity (Supplementary Figure S5). To confirm this speculation for HR cell death mediated by OsNAC4, it is important to clarify the phosphorylation site of OsNAC4 during HR cell death, the relationship between phosphorylation of OsNAC4 and HR cell death induction and the direct participation of IREN in DNA fragmentation during HR cell death.

Materials and methods

Protoplast preparation and gene transformation

Rice protoplasts were isolated from Oc cultured cells and PEG-mediated transformation was performed as described previously (Takai *et al*, 2006). Detailed condition of this experiment is described in Supplementary data.

Detection of HR cell death in cultured rice cells

HR cell death in cultured rice cells was detected by Evans blue staining as described previously (Che *et al*, 1999). Detailed condition for detection of HR cell death is described in Supplementary data.

Generation of transgenic rice cells using RNAi constructs specific for OsNAC4

We used a pANDA vector (Miki and Shimamoto, 2004) to express inverted repeat sequences of a 501-bp fragment of the *OsNAC4* gene. The target sequence was initially amplified by PCR; the resulting PCR product was cloned into the pENTR/D-TOPO cloning vector (Invitrogen). The target sequence was transferred into the pANDA vector by an LR clonase reaction. The construct was then introduced into *Agrobacterium tumefaciens* EHA105 by electroporation, followed by *Agrobacterium*-mediated transformation of rice.

Microarray data analysis

A long oligonucleotide array (60-mer; Agilent Technologies, 22 K) designed by the Institute for Genomic Research from tentative consensus sequences was used in this study. We used ArrayVision 5.1 (Amersham) and GeneSpring GX 7.3 (Silicon Genetics, Redwood, CA, USA) software for microarray data analysis. Two-way ANOVA was applied to determine the expressed sets of genes. Statistical significances were adjusted by multiple testing correction (Benjamini-Hochberg False Discovery Rate, 0.01). To determine the differentially expressed genes from the selected genes between NR2-4 and control line during HR, *t*-test was used. The detailed conditions for these experiments are described in Supplementary data.

RNA isolation and quantitative real-time RT–PCR

Total RNA was isolated from cultured rice cells using an RNeasy Plant Mini Kit (QIAGEN, Hilden, Germany) with DNase digestion process according to the manufacturer's instructions. Quantitative real-time RT–PCR was performed on an Opticon2 (Bio-Rad, Biorad, Hercules, CA) using a QuantiTect SYBR Green RT–PCR Kit (QIAGEN). Detailed condition of real-time RT–PCR is described in Supplementary data.

Nuclei purification and immunoblotting analysis

Nuclei and cytosol fractions were purified from rice protoplasts. Isolated nuclear fraction and cytosol fraction were separated by SDS-polyacrylamide gels and electrophoretically transferred to a nitrocellulose membrane (Millipore, Bedford, USA). OsNAC4 was detected by specific anti-OsNAC4 antibody. Detailed condition of these experiments is described in Supplementary data.

Immunoprecipitation

Anti-OsNAC4 antibody were added to the isolated cytosol and nuclei fractions and incubated for 6 h, followed by the addition of Protein A-sepharose (GE Healthcare). The protein A-sepharose precipitates were washed with binding buffer and resuspended in 30 μl Laemmli sample buffer. Equal quantities of protein samples were loaded on SDS–PAGE gel and analysed by immunoblotting. Detailed condition of these experiments is described in Supplementary data.

Supplementary data

Supplementary data are available at *The EMBO Journal* Online (http://www.embojournal.org).

Acknowledgements

We are grateful to Eriko Okamoto and Hiromi Morii for their excellent technical support. This work was supported in part by Grants-in-Aid for Scientific Research (B) (19380067) and Creative Scientific Research (16GS0316 to AI) from the Ministry of Education, Culture, Sports, Science and Technology of Japan.

References

Alvarez ME, Pennell RI, Meijer PJ, Ishikawa A, Dixon RA, Lamb C (1998) Reactive oxygen intermediates mediate a systemic signal network in the establishment of plant immunity. *Cell* **92:** 773–784

Che FS, Iwano M, Tanaka N, Takayama S, Minami E, Shibuya N, Kadota I, Isogai A (1999) Biochemical and morphological features of rice cell death induced by *Pseudomonas avenae*. *Plant Cell Physiol* **40:** 1036–1045

Che FS, Nakajima Y, Tanaka N, Iwano M, Yoshida T, Takayama S, Kadota I, Isogai A (2000) Flagellin from an incompatible strain of *Pseudomonas avenae* induces a resistance response in cultured rice cells. *J Biol Chem* **275:** 32347–32356

Collinge M, Boller T (2001) Differential induction of two potato genes, Stprx2 and StNAC, in response to infection by Phytophthora infestans and to wounding. *Plant Mol Biol* **46:** 521–529

Cornejo MJ, Luth D, Blankenship KM, Anderson OD, Blechl AE (1993) Activity of a maize ubiquitin promoter in transgenic rice. *Plant Mol Biol* **23:** 567–581

Dong A, Liu Z, Zhu Y, Yu F, Li Z, Cao K, Shen WH (2005) Interacting proteins and differences in nuclear transport reveal specific functions for the NAP1 family proteins in plants. *Plant Physiol* **138:** 1446–1456

Fujita M, Fujita Y, Maruyama K, Seki M, Hiratsu K, Ohme-Takagi M, Tran LS, Yamaguchi-Shinozaki K, Shinozaki K (2004) A dehydration-induced NAC protein, RD26, is involved in a novel ABA-dependent stress-signaling pathway. *Plant J* **39:** 863–876

Fujiwara S, Tanaka N, Kaneda T, Takayama S, Isogai A, Che FS (2004) Rice cDNA microarray-based gene expression profiling of the response to flagellin perception in cultured rice cells. *Mol Plant Microbe Interact* **17:** 986–998

Hatsugai N, Kuroyanagi M, Yamada K, Meshi T, Tsuda S, Kondo M, Nishimura M, Hara-Nishimura I (2004) A plant vacuolar protease, VPE, mediates virus-induced hypersensitive cell death. *Science* **305:** 855–858

Hegedus D, Yu M, Baldwin D, Gruber M, Sharpe A, Parkin I, Whitwill S, Lydiate D (2003) Molecular characterization of *Brassica napus* NAC domain transcriptional activators induced in response to biotic and abiotic stress. *Plant Mol Biol* **53:** 383–397

Jones JD, Dangl JL (2006) The plant immune system. *Nature* **444:** 323–329

Kadota I, Mizuno A, Nishiyama K (1996) Detection of a protein specific to the strain of *Pseudomonas avenae* Manns 1909 pathogenic to rice. *Ann Phytopathol Soc Jpn* **62:** 425–428

Kaneda T, Fujiwara S, Takai R, Takayama S, Isogai A, Che FS (2007) Identification of genes involved in induction of plant hypersensitive cell death. *Plant Biotech* **24:** 191–200

Krishna P, Gloor G (2001) The HSP90 family of proteins in Arabidopsis thaliana. *Cell Stress Chaperones* **6:** 238–246

Kutuk O, Basaga H (2006) Bcl-2 protein family: implications in vascular apoptosis and atherosclerosis. *Apoptosis* **11:** 1661–1675

Lam E (2004) Controlled cell death, plant survival and development. *Nat Rev Mol Cell Biol* **5:** 305–315

Levine A, Pennell RI, Alvarez ME, Palmer R, Lamb C (1996) Calcium-mediated apoptosis in a plant hypersensitive disease resistance response. *Curr Biol* **6:** 427–437

McCabe PF, Levine A, Meijer PJ, Tapon NA, Pennell RI (1997) A programmed cell death pathway activated in carrot cells cultured at low cell density. *Plant J* **12:** 267–280

Miki D, Shimamoto K (2004) Simple RNAi vectors for stable and transient suppression of gene function in rice. *Plant Cell Physiol* **45:** 490–495

Mindrinos M, Katagiri F, Yu GL, Ausubel FM (1994) The *A. thaliana* disease resistance gene RPS2 encodes a protein containing a nucleotide-binding site and leucine-rich repeats. *Cell* **78:** 1089–1099

Mittler R, Shulaev V, Lam E (1995) Coordinated activation of programmed cell death and defense mechanisms in transgenic tobacco plants expressing a bacterial proton pump. *Plant Cell* **7:** 29–42

Ooka H, Satoh K, Doi K, Nagata T, Otomo Y, Murakami K, Matsubara K, Osato N, Kawai J, Carninci P, Hayashizaki Y, Suzuki K, Kojima K, Takahara Y, Yamamoto K, Kikuchi S (2003) Comprehensive analysis of NAC family genes in *Oryza sativa* and *Arabidopsis thaliana*. *DNA Res* **10:** 239–247

Picard D (2002) Heat-shock protein 90, a chaperone for folding and regulation. *Cell Mol Life Sci* **59:** 1640–1648

Richberg MH, Aviv DH, Dangl JL (1998) Dead cells do tell tales. *Curr Opin Plant Biol* **1:** 480–485

Shi Y (2002) Mechanisms of caspase activation and inhibition during apoptosis. *Mol Cell* **9:** 459–470

Souer E, van Houwelingen A, Kloos D, Mol J, Koes R (1996) The no apical meristem gene of Petunia is required for pattern formation in embryos and flowers and is expressed at meristem and primordia boundaries. *Cell* **85:** 159–170

Tajima H, Iwata Y, Iwano M, Takayama S, Koizumi N (2008) Identification of an Arabidopsis transmembrane bZIP transcription factor involved in the endoplasmic reticulum stress response. *Biochem Biophys Res Commun* **374:** 242–247

Takabatake R, Ando Y, Seo S, Katou S, Tsuda S, Ohashi Y, Mitsuhara I (2007) MAP kinases function downstream of HSP90 and upstream of mitochondria in TMV resistance gene N-mediated hypersensitive cell death. *Plant Cell Physiol* **48:** 498–510

Takai R, Kaneda T, Isogai A, Takayama S, Che FS (2006) A new method for defense response analysis using a transient expression system in rice. *Biosci Biotech Biochem* **71:** 590–593

Tanaka N, Nakajima Y, Kaneda T, Takayama S, Che FS, Isogai A (2001) DNA laddering during hypersensitive cell death in cultured rice cells induced by an incompatible strain of Pseudomonas avenae. *Plant Biotech* **18:** 295–299

Yao N, Tada Y, Park P, Nakayashiki H, Tosa Y, Mayama S (2001) Novel evidence for apoptotic cell response and differential signals in chromatin condensation and DNA cleavage in victorin-treated oats. *Plant J* **28:** 13–26

